Research Square

Preprints are preliminary reports that have not undergone peer review.
They should not be considered conclusive, used to inform clinical practice,
or referenced by the media as validated information.

Detection of QTLs for Mesocotyl and Coleoptile Traits Related to Maize Soil Emergence Ability

Bu Lin
Guizhou University
Xiaolan Hu
Guizhou University
Hanlei Wang
Guizhou University
Hongbo Qiu
qhb001122@163.com

Guizhou University
Xiaomei Zhang
Center for Agricultural Technology Extension of Dehong Prefecture

Research Article

Keywords: Maize, Seedling emergence, Coleoptile, Mesocotyl, Quantitative trait loci (QTL)

Posted Date: May 28th, 2026

DOI: https://doi.org/10.21203/rs.3.rs-9637957/v1

License: This work is licensed under a Creative Commons Attribution 4.0 International License.
Read Full License

Additional Declarations: No competing interests reported.

Abstract

Insufficient soil emergence ability of maize is a critical agronomic defect that restricts seedling emergence efficiency, severely threatening population emergence uniformity, field seedling establishment rate, and mechanized sowing emergence quality in tropical and subtropical rainfed agricultural areas. To elucidate the genetic basis of soil emergence ability in maize, a population of 119 F_2 individuals derived from a cross between maize inbred lines T32 and J51 was employed as the mapping population. We constructed a genetic linkage map comprising 152 SSR markers, which spanned 1357.42 cM of the genome with an average marker density of 8.9 cM. Coleoptile and mesocotyl lengths, as key traits for seedling emergence ability, were measured in the $F_{2:3}$ population across three distinct environments (glasshouse, Huaxi, and Gaofeng). Significant phenotypic variation for seedling emergence was observed between the parental lines. We identified a total of nineteen QTLs associated with these traits across the environments: nine in the glasshouse, six in Huaxi, and four in Gaofeng. Notably, two stable QTLs were consistently detected across all three environments on chromosome 3: one for coleoptile length, flanked by markers umc2262–umc2033 (position 3.04), and the other for mesocotyl length, flanked by markers umc1052–umc2050 (positions 3.07–3.09). The additive effects at these loci were contributed by the maternal parent, J51. These stable QTLs represent valuable targets for the fine mapping of genes underlying seedling vigor and for marker-assisted selection in maize breeding programs.

1 Introduction

Maize (Zea mays L.) stands as a cornerstone of global food security. In China, it accounted for approximately 38.9% of the total grain output in 2020, with a production of 261 million tons. Between 2010 and 2020, the annual growth rate of maize yield was 2.66%, driven almost equally by area expansion (53.6%) and yield improvement (46.4%) (Chou et al., 2021). The Southwest region of China is a major historical and strategic zone for maize production. As the nation's third-largest maize-producing area, it contributes about 14.1% of the total planting area and 11.4% of the national output, with an annual sown area consistently over 4.67 million hectares (Dang et al., 2016; Luo et al., 2017).However, productivity in this region is severely constrained by a challenging agronomic environment characterized by complex topography, variable climate, and frequent natural disasters. A primary limiting factor is widespread soil crusting (Li et al., 2016), which significantly increases mechanical impedance to emerging seedlings. This physical barrier often interacts with moisture stress—either drought or waterlogging—creating a potent combined abiotic stress that severely compromises crop establishment (Whalley et al., 1999). The resulting reduction in emergence rate and poor stand uniformity is a well-documented cause of substantial yield loss (Botta et al., 2004). Beyond the physical impediment, soil crusting degrades soil structure, reduces water and nutrient retention, and can persist for extended periods (Brais, 2001), and alters pH, frequently inducing nutrient deficiencies (e.g., nitrogen, phosphorus, magnesium) that further limit plant growth and final yield quality (Wang et al., 2018).While agronomic interventions such as soil amendments have shown some efficacy in alleviating crusting and improving emergence in other crops (Han et al., 2022), genetic improvement remains the most sustainable strategy

for addressing this stress. Consequently, improving the genetic capacity of maize to penetrate crusted soil and establish vigorous stands is a critical breeding objective for stabilizing and enhancing productivity in this region and similar stress-prone environments worldwide.

The ability of seedlings to emerge is primarily determined by the elongation of the mesocotyl and coleoptile, which are distinct underground organs of the grass seedling that play a critical role in pushing the shoot through the soil (Hoshikawa, 1969).In a seminal study, Allan et al. (1962) demonstrated that coleoptile length was a key determinant of seedling emergence in fall-sown wheat, highlighting the fundamental role of this organ in pushing the shoot through the soil. Their correlation analysis identified mesocotyl and coleoptile elongation as the key factors for successful seedling emergence through soil. Subsequent physiological studies have further revealed that mesocotyl elongation is regulated by endogenous hormones, particularly gibberellins and auxins (Du et al., 2008).

Early agronomic investigations documented the detrimental effects of extremely deep planting on maize stand establishment (Dungan, 1950). Subsequent research has further explored the genetic and molecular basis of germination-related traits under various conditions. For instance, Ye et al. (2019) found that the ZmMYB59 gene was down-regulated under deep sowing. They hypothesized a negative regulatory role for this gene in soil penetration during germination. Through Agrobacterium-mediated transformation, they obtained T3-generation overexpressing lines and conducted experiments under different sowing depths, abiotic stresses, and hormone treatments. Their results suggested that ZmMYB59 likely acts as a negative regulator, possibly linked to the gibberellin metabolism pathway. Similarly, Sun et al. (2019) demonstrated that overexpression of ZmCOL9 effectively promoted mesocotyl elongation and significantly improved the deep-sowing emergence capacity of transgenic maize, providing direct evidence for genetic engineering approaches to enhance emergence vigor.Quantitative trait locus (QTL) mapping has also been employed to dissect these complex traits. Under two sowing depths (12.5 cm and 2 cm), Liu et al. (2017) identified 65 QTLs for germination-related traits, including those for mesocotyl and coleoptile length. Using a recombinant inbred line population under 12.5 cm sowing depth, Han et al. (2020) mapped 31 QTLs for related traits. Zhang et al. (2012) reported 25 QTLs under 10 cm and 20 cm sowing depths. These studies collectively confirm that traits like mesocotyl and coleoptile length are quantitatively inherited.In addition, germplasm evaluation studies have identified substantial genetic variation for deep-sowing tolerance among maize inbred lines, providing valuable resources for genetic dissection (Zhang et al., 2007). However, discrepancies among the reported QTLs highlight the influence of differing genetic materials, experimental conditions, and methodologies.It is crucial to note that the aforementioned studies predominantly focus on tolerance to deep sowing, a stress condition largely associated with energy reserve mobilization and hypoxic response. In contrast, soil crusting presents a distinct challenge characterized by direct physical mechanical impedance, which has been shown to affect root architecture and seedling growth across diverse plant species (Alameda & Villar, 2009), compromise seedling establishment in natural and managed ecosystems (Bassett et al., 2005), and independently and severely inhibit root development and crop productivity (Colombi et al., 2017). Research specifically investigating maize seedling emergence capacity under soil crusting conditions remains notably scarce.

2 Materials and methods

2.1 Plant material and field sites

Based on prior field evaluations and comprehensive agronomic performance, two maize inbred lines, T32 and J51, were selected as parental lines to construct a mapping population. J51 is an elite local inbred line from Guizhou Province, China, characterized by good grain quality, high yield, strong adaptability. It has been observed to exhibit superior soil penetration ability and germination vigor under local cultivation conditions. T32 is a breeding line derived from Suwan1C9, a tropical germplasm of Thai origin. An F_2 mapping population was developed by crossing J51 (used as the female parent) with T32 (as the male parent). The F_2 individuals were subsequently self-pollinated to generate $F_{2:3}$ families, which were used for phenotypic evaluation. The final mapping population consisted of 119 $F_{2:3}$ families derived from this cross.The hybrid J51 × T32 was made in Guiyang in the spring of 2019. The F_1 generation was grown and self-pollinated in Sanya, Hainan, during the winter of 2019 to produce F_2 ears. In the spring of 2021, the F_2 population was planted in Guiyang and selfed to obtain $F_{2:3}$ families. Based on ear integrity and seed availability, 119 $F_{2:3}$ families were selected and planted for this study in 2022.

2.2 Phenotypic evaluation under field and controlled conditions

Phenotypic assessment was conducted across three environments: a controlled glasshouse at the College of Agriculture, Guizhou University; and two field sites prone to natural soil crusting in Gaofeng Town, Anshun City, and Huaxi District, Guiyang City, Guizhou Province, China.

2.2.1 Glasshouse experiment with induced soil crusting

To impose controlled soil crusting stress, $F_{2:3}$ families were sown in seedling trays in the glasshouse. A loam soil with high crusting potential was collected from the university farm, sieved through a 1.5 mm mesh to destroy natural aggregates, and autoclaved to eliminate pathogens and weed seeds. After cooling, seeds were sown at a depth of 2.5 cm. Crust formation was induced by irrigation with slightly alkaline tap water post-sowing, followed by placement in a location with moderate light and restricted air circulation to facilitate surface hardening. The experiment was maintained at 20°C and 60% relative humidity with two replications. Fifteen seeds per family were sown per replicate. Emergence rate was scored 15 days after sowing. At the two-leaf stage, mesocotyl length (from the scutellar node to the coleoptile base) and coleoptile length were measured. Mean values per family were used for analysis.

2.2.2 Field experiments in natural crusting-prone environments

Field trials were established at two locations representative of the karst plateau region of Guizhou, characterized by a subtropical monsoon climate with intense, episodic rainfall. This weather pattern,

combined with specific soil properties, promotes natural soil crusting through raindrop impact and surface runoff, which disrupts aggregates and seals the soil surface upon drying.

- **Gaofeng Town (Anshun)**: Situated in a hilly basin of the eastern Yunnan-Guizhou Plateau (elevation 1,250–1,350 m) with typical karst topography.
- **Huaxi District (Guiyang)**: Located on the eastern slope of the Yunnan-Guizhou Plateau. The soils, derived from limestone parent material, are clay-rich, alkaline to neutral, and have poor structure, making them highly susceptible to crusting.

A randomized complete block design with two replications was used at both sites. Each plot consisted of a single 4.5 m row with 0.6 m row spacing and 0.35 m hill spacing, with two plants retained per hill after thinning. Phenotypic traits were evaluated at the two-leaf stage, and plot means were calculated for each family.

2.3 Phenotypic data analysis

At the two-leaf stage, the mean mesocotyl and coleoptile lengths of all plants within a plot were calculated to represent the plot value. The average of the two replicate plots was then used as the phenotypic value for each family. Data normality was assessed using SPSS 20.0.

For single-environment analyses across the three tested locations, a one-way analysis of variance (ANOVA) based on a randomized complete block design was applied. Combined analysis across all environments was performed using a two-way ANOVA with a randomized complete block design, considering both genotype and environment as factors.

Broad-sense heritability (H^2) was estimated on an entry-mean basis. The genotypic variance component was derived from the variance among families, while the error variance component from the ANOVA was treated as the environmental variance. Heritability was calculated as $H^2 = (\sigma^2_G) / (\sigma^2_G + \sigma^2_E/n)$, where σ^2_G is the genotypic variance, σ^2_E is the environmental variance, and *n* is the number of environments.

2.4 Construction of the genetic linkage map

Genomic DNA was extracted from the F_2 population using the cetyltrimethylammonium bromide (CTAB) method. Genotyping was performed via 10% non-denaturing polyacrylamide gel electrophoresis. A genotype database for the 119 F_2 individuals was constructed as a two-way table in Microsoft Excel, with individual plant IDs listed by row and simple sequence repeat (SSR) marker names by column.SSR markers have been widely employed in maize genetic studies owing to their codominant inheritance, high reproducibility, and genome-wide coverage (Wu & Lu, 2020).The linkage map was developed using JoinMap version 4.0. SSR markers were grouped at a logarithm of odds (LOD) threshold ≥ 3.0. Recombination frequencies between linked loci were converted to genetic distances in centimorgans (cM) using the Kosambi mapping function.

2.5 Genetic map construction and QTL mapping

QTL analysis was performed using the inclusive composite interval mapping (ICIM) method implemented in the QTL IciMapping version 4.0 software (Wang et al., 2009; Li et al., 2007, 2008). A walk speed of 1 cM and a manually set LOD threshold of 2.0 (corresponding to a significance level of $P < 0.05$) were used for scanning. Missing data were excluded from the analysis.

A putative QTL was declared when the LOD score profile within a marker interval exceeded the threshold, with the peak LOD position considered the QTL location. For each detected QTL, the percentage of phenotypic variance explained (PVE) as well as its additive and dominance effects were estimated. The mode of gene action was determined based on the absolute value of the dominance-to-additive effect ratio (|d/a|), following established criteria (Stuber et al., 1987; Tuberosa et al., 1998): additive (A) for |d/a| = 0–0.20, partial dominance (PD) for 0.21–0.80, dominance (D) for 0.81–1.20, and overdominance (OD) for values > 1.20.

3 Result

3.1 Significant differences between parental lines

Analysis of variance revealed highly significant differences ($P < 0.01$) in key emergence-related traits between the two parental lines across all experimental treatments. As presented in Table 3, both mesocotyl length and coleoptile length of J51 were significantly greater than those of T32 under each condition.

The emergence rate further confirmed this phenotypic divergence. J51 consistently achieved a high emergence rate of 90% in the glasshouse, Gaofeng, and Huaxi environments. In contrast, the emergence rate of T32 was 60% in both the glasshouse and Gaofeng, and decreased to 50% in Huaxi.In conclusion, the parental line J51 exhibits significantly superior performance in both morphological traits (mesocotyl and coleoptile length) and the ultimate emergence rate compared to T32, confirming its strong soil-penetration capacity.

3.2 Phenotypic variation in maize mesocotyl and coleoptile

Field evaluation across the three environments (glasshouse, Huaxi, and Gaofeng) consistently demonstrated distinct emergence capacities between the parental lines. The inbred line J51 exhibited superior emergence performance, while T32 showed consistently poor emergence across all sites.

Normality tests on the mean trait values of the 119 $F_{2:3}$ families indicated no significant deviation from a normal distribution, with absolute values for both skewness and kurtosis coefficients being less than 1 (Tables 1 and 2). This confirms that the data meet a fundamental assumption for QTL mapping analysis. The frequency distributions for both mesocotyl and coleoptile length were continuous, which is characteristic of quantitative traits controlled by multiple genes. Notably, the presence of pronounced peaks in these distributions suggests the potential influence of major-effect quantitative trait loci (QTLs) underlying the variation in these traits.

3.3 Analysis of variance

Variance analysis was performed on mesocotyl length and coleoptile length across three environments. The results indicated that differences among locations were highly significant for both traits (mesocotyl: F = 6.309, P = 0.0001; coleoptile: F = 157.554, P = 0.0001), suggesting that the emergence ability of the same family varied significantly across different locations. Significant differences among families were observed for mesocotyl length (F = 3.860, P = 0.005), while differences among families for coleoptile length were highly significant (F = 132.920, P = 0.0001). This indicates that emergence ability also differed among different families. The interaction between location and family reached a significant level for mesocotyl length (F = 1.235, P = 0.005) and a highly significant level for coleoptile length (F = 13.580, P = 0.0001), demonstrating that the performance of the same family was inconsistent across locations, with a significant genotype-by-environment interaction effect. The ANOVA results collectively indicate that maize emergence ability is influenced not only by genetic materials and environmental conditions but also by their interaction. Based on data from the three locations, the estimated heritability for stress resistance was 69.9% for mesocotyl length and 74.26% for coleoptile length, revealing that stress resistance is primarily controlled by genetic factors.

3.4 Genetic linkage map construction

A total of 1,380 SSR primer pairs, located in different bin positions across all ten maize chromosomes, were selected based on information from MaizeGDB (http://www.maizegdb.org/). These primers were initially screened for polymorphism between the two parental lines, T32 and J51. Among them, 194 pairs (14.05%) revealed clear polymorphisms. These polymorphic primers were then used for genotyping the F_2 mapping population.

Subsequently, 152 high-quality SSR markers showing consistent and clear polymorphisms were chosen for comprehensive linkage analysis. Genotypic data from the F_2 population obtained with these 152 markers were analyzed using JoinMap version 4.0. A genetic linkage map was successfully constructed, comprising ten linkage groups corresponding to the ten chromosomes. This map integrated all 152 SSR loci, with 13 to 18 markers per chromosome (average of 15.2). The total map length spanned 1357.42 cM, with an average interval of 8.9 cM between adjacent markers (Table 6). The order of most markers was consistent with their positions on the standard reference map. Minor local discrepancies observed for a few markers were likely attributable to the specific genetic background of the plant materials used in this study.

3.5 QTL mapping and genetic effect analysis

QTL analysis for mesocotyl length and coleoptile length was performed based on the investigation of topsoil emergence capacity in $F_{2:3}$ families across three experimental sites (Tables 7 & 8). A total of 10 QTLs were detected for mesocotyl length. For coleoptile length, a total of nine QTLs were detected across the three environments. Among them, a QTL located in the marker interval *umc1052–umc2050* on chromosome 3 (bin 3.07–3.09) was consistently detected in all three environments.

In the glasshouse environment, five QTLs were detected for mesocotyl length. Their genetic positions were 135.00 cM (designated *WSMES1a*), 15.00 cM (*WSMES3a*), 186.00 cM (*WSMES4a*), 46.00 cM (*WSMES8a*), and 103.00 cM (*WSMES9a*) on chromosomes 1 (bin 1.10–1.11), 3 (bin 3.07–3.09), 4 (bin 4.10–4.11), 8 (bin 8.05–8.06), and 9 (bin 9.05–9.06), respectively. The QTL *WSMES1a* was flanked by markers *bnlg1347a* and *umc1538a*, with an additive effect of -0.107. The allele for this QTL was inherited from parent T32, explaining 4.284% of the phenotypic variation. The QTL *WSMES3a* was located between *umc1052* and *umc2050*, exhibiting an additive effect of 0.108 from parent J51, which accounted for 10.466% of the phenotypic variation. The QTL *WSMES4a* was flanked by *bnlg1890* and *bnlg1917*, showing an additive effect of 0.140 from parent J51 and explaining 5.783% of the phenotypic variation. The QTL *WSMES8a* was located between *bnlg1607* and *bnlg2181*, with an additive effect of -0.040 from parent T32, explaining 4.443% of the phenotypic variation. The QTL *WSMES9a* was flanked by *umc1657* and *umc2346*, having an additive effect of -0.128, with the allele contributed by parent T32, which explained 6.617% of the phenotypic variation.

At the Huaxi site, three QTLs were identified for mesocotyl length, located on chromosomes 1 (bin 1.09–1.10), 3 (bin 3.07–3.09), and 7 (bin 7.00–7.01). Their genetic positions were 126.00 cM (*HXMES1a*), 16.00 cM (*HXMES3a*), and 8.00 cM (*HXMES7a*), respectively. The QTL *HXMES1a* was flanked by markers *umc1715* and *bnlg1347a*, with an additive effect of 0.008 from parent J51, explaining 5.598% of the phenotypic variation. The QTL *HXMES3a* was located between *umc1052* and *umc2050*, exhibiting an additive effect of 0.211 from parent J51, which accounted for 15.516% of the phenotypic variation. The QTL *HXMES7a* was flanked by *bnlg1367* and *umc1159*, showing an additive effect of 0.081 from parent J51 and explaining 10.571% of the phenotypic variation.

At the Gaofeng site, two QTLs were detected for mesocotyl length on chromosomes 3 (bin 3.07–3.09) and 7 (bin 7.00–7.01). Their genetic positions were 16.00 cM (*GFMES3a*) and 8.00 cM (*GFMES7a*), respectively. The QTL *GFMES3a* was flanked by markers *umc1052* and *umc2050*, with an additive effect of 0.288 from parent J51, explaining 16.157% of the phenotypic variation. The QTL *GFMES7a* was located between *bnlg1367* and *umc1159*, exhibiting an additive effect of -0.281 from parent T32, which accounted for 9.397% of the phenotypic variation.

For coleoptile length, four QTLs were detected in the glasshouse environment, located on chromosomes 1, 3, 6, and 8. Their genetic positions were 30.00 cM (*WSCOL1a*), 111.00 cM (*WSCOL3a*), 74.00 cM (*WSCOL6a*), and 41.00 cM (*WSCOL8a*), respectively. These QTLs were flanked by marker intervals *umc1144–dupssr26*, *umc2262–umc2033*, *bnlg1812–umc1130*, and *bnlg1607–bnlg2181*, respectively. The QTL *WSCOL6a* on chromosome 6 showed an additive effect of -0.013, with the allele contributed by parent T32, explaining 6.681% of the phenotypic variation. The additive effects for the other three QTLs (*WSCOL1a*, *WSCOL3a*, and *WSCOL8a*) were all from parent J51, with values ranging from 0.054 to 0.082, and they explained 5.685% to 10.059% of the phenotypic variation.

At the Huaxi site, three QTLs were identified for coleoptile length on chromosomes 3, 4, and 7. Their genetic positions were 111.00 cM (*HXCOL3a*), 160.00 cM (*HXCOL4a*), and 118.00 cM (*HXCOL7a*),

respectively. These QTLs were flanked by marker intervals *umc2262–umc2033*, *umc1101–bnlg1337*, and *bnlg1666–umc1944*, respectively. The additive effects for all three QTLs were from parent J51, with values of 0.095, 0.081, and 0.090, explaining 10.971%, 7.876%, and 7.080% of the phenotypic variation, respectively.

At the Gaofeng site, two QTLs were detected for coleoptile length on chromosomes 1 and 3. Their genetic positions were 30.00 cM (*GFCOL1a*) and 116.00 cM (*GFCOL3a*), respectively. These QTLs were flanked by marker intervals *umc1144–dupssr26* and *umc2262–umc2033*, respectively. The additive effects for both QTLs were from parent J51, with values of 0.079 and 0.097, explaining 7.080% and 12.251% of the phenotypic variation, respectively.

Comparative analysis of the mapping results from the three environments identified two stable QTLs that were consistently expressed across all locations.

The first stable QTL, corresponding to WSCOL3a (greenhouse), HXCOL3a (Huaxi), and GFCOL3a (Gaofeng), was mapped to chromosome 3 within the marker interval umc2262–umc2033 (bin 3.04). Its genetic position ranged from 111 to 116 cM across environments. The LOD scores were 3.266, 3.577, and 4.097 in the greenhouse, Huaxi, and Gaofeng environments, respectively. This QTL explained 10.059% to 12.251% of the phenotypic variation. The gene action was partial dominance, with the increasing allele consistently contributed by the maternal parent J51.The second stable QTL, corresponding to WSMES3a, HXMES3a, and GFMES3a, was also located on chromosome 3 within the marker interval umc1052–umc2050 (bins 3.07–3.09). Its genetic position ranged from 15 to 16 cM. The LOD scores were 3.778, 4.825, and 5.021 for the greenhouse, Huaxi, and Gaofeng sites, respectively. This QTL explained a larger proportion of phenotypic variation, ranging from 10.466% to 16.157%. The gene action was additive/dominant, and the increasing allele was also derived from the maternal parent J51.

3.6 Joint analysis

A joint QTL analysis was performed for coleoptile length using data integrated from the three experimental sites (Table 9). A total of 10 QTLs were detected, distributed on chromosomes 1, 2, 3, 4, 5, 6, and 9. The LOD scores for these QTLs ranged from 2.837 to 11.696, explaining 1.311% to 9.686% of the phenotypic variation. The stable QTL on chromosome 3 (flanked by markers *umc2262–umc2033*), which was expressed across all three environments in the single-environment analysis, was also identified in this joint analysis.

Similarly, a joint QTL analysis for mesocotyl length across the three environments was conducted (Table 10). Ten QTLs were identified, located on chromosomes 1, 2, 3, 4, 5, 6, 7, 8, and 9. Their LOD scores ranged from 2.086 to 10.410, accounting for 1.180% to 13.562% of the phenotypic variation. The consistent QTL on chromosome 3 (within the marker interval *umc1052–umc2050*), detected in all single environments, was also recovered in the joint analysis.

Notably, these stable QTLs identified in both the single-environment and joint analyses were mapped to the same chromosomal regions. They exhibited significantly higher LOD scores and phenotypic contributions compared to other QTLs. This strongly indicates their stable expression and suggests a tight genetic linkage with the target gene(s). Consequently, these genomic regions represent promising candidate intervals for marker-assisted selection in maize topsoil emergence capacity.

Furthermore, several QTLs detected in the joint analysis were not observed in any single-environment analysis. These QTLs likely have minor effects on topsoil emergence capacity and may only be detectable when statistical power is increased through data integration from multiple environments.

Discussion

While the genetic and physiological mechanisms underlying seedling emergence through compacted soil have been extensively studied in rice (e.g., Zhang et al., 2005; Xu et al., 2015) and successfully applied in breeding, related research in maize remains relatively limited. In this study, we not only conducted rigorous laboratory experiments simulating soil compaction but also performed field evaluations in regions prone to this condition, based on extensive practical experience, which yielded stable and reliable results. Two optimal sites for natural field evaluation were identified: Huaxi District, Guiyang City, and Gaofeng Town, Anshun City, both located in the karst region of central Guizhou Province. These sites share highly similar climatic conditions, including an average annual temperature (~ 14°C), annual precipitation (~ 1200 mm), and average humidity (~ 80%). This humid, rainy climate is a key driver of soil compaction: intensive summer rainfall directly impacts the soil surface, promoting crust formation, while prolonged high humidity accelerates the decomposition of soil organic matter, reducing its resistance to compaction.

In this study, the mesocotyl and coleoptile lengths of 119 $F_{2:3}$ families across three environments all followed a normal distribution. The parental lines used were elite inbreds J51 and T32, which exhibited significant differences in the target traits (mesocotyl and coleoptile length), making them suitable for constructing a mapping population. The genetic map constructed here integrated 152 markers. However, certain regions on some chromosomes were not covered by markers, and the genetic distances between some markers were relatively large. This may be due to uneven recombination frequencies across chromosomal regions or a lack of polymorphism between the parents in those intervals, warranting further investigation. Future work should aim to saturate these gaps with additional markers to reduce map distances and ultimately identify markers tightly linked to major QTLs. This would facilitate marker-assisted selection (MAS) for maize topsoil emergence capacity, help elucidate its genetic basis, and support the development and improvement of germplasm with high and uniform emergence rates under compacted soil conditions.

In the greenhouse environment, this study detected four QTLs for coleoptile length on chromosomes 1 (bin 1.04–1.05), 3 (bin 3.04), 6 (bin 6.02–6.03), and 8 (bin 8.05–8.06), and five QTLs for mesocotyl length on chromosomes 1 (bin 1.10–1.11), 3 (bin 3.07–3.09), 4 (bin 4.10–4.11), 8 (bin 8.05–8.06), and 9 (bin

9.05–9.06). At the Huaxi site, three QTLs for coleoptile length were identified on chromosomes 3 (bin 3.04), 4 (bin 4.09–4.11), and 7 (bin 7.04), and three QTLs for mesocotyl length were found on chromosomes 1 (bin 1.09–1.10), 3 (bin 3.07–3.09), and 7 (bin 7.00–7.01). At the Gaofeng site, two QTLs for coleoptile length were detected on chromosomes 1 (bin 1.04–1.05) and 3 (bin 3.04), and two QTLs for mesocotyl length were mapped to chromosomes 3 (bin 3.07–3.09) and 7 (bin 7.00–7.01).

Notably, QTLs associated with coleoptile length flanked by *umc1144–dupssr26* were co-detected in two environments. For mesocotyl length, chromosomal intervals sharing the marker *bnlg1347a*—specifically *bnlg1347a–umc1538a* and *umc1715–bnlg1347a*—were identified in both the greenhouse and Huaxi environments. These genomic regions hold significant reference value for future in-depth research on maize topsoil emergence capacity.

Furthermore, QTLs related to stress tolerance emergence capacity on chromosome 3 were consistently detected across all three environments (greenhouse, Huaxi, and Gaofeng). These stable QTLs exhibited relatively high LOD scores and phenotypic contribution rates, indicating that the inbred line J51 possesses genetic factors conferring resilience. This stability across diverse environments underscores their potential value for breeding applications.

Conclusion

This study identified 19 QTLs associated with topsoil emergence capacity across three environments. Notably, two stable, co-localized QTLs on chromosome 3—flanked by markers *umc2262* and *umc2033*, and *umc1052* and *umc2050*, respectively—were consistently detected in all environments. For coleoptile length, they explained 10.059%, 10.971%, and 12.251% of the phenotypic variation, with additive effects of 0.0733, 0.095, and 0.097, respectively. For mesocotyl length, they accounted for 10.466%, 15.516%, and 16.157% of the variation, with additive effects of 0.108, 0.211, and 0.288, respectively. All additive effects were contributed by the maternal parent J51.

Research on maize topsoil emergence capacity remains limited domestically. Mapping these resilience-related genes facilitates the selection of elite germplasm and enriches the genetic resource pool for stress tolerance. The findings of this study provide a valuable case reference for related research, offer a theoretical basis and material support for marker-assisted selection, establish a foundation for the efficient transfer of resilience genes, and supply a theoretical framework for in-depth exploration of the genetic mechanisms underlying topsoil emergence in maize.

Abbreviations

QTL Quantitative trait loci

MES Mesocotyl

COL Coleoptile

HX HuaXi

GF GaoFeng

WS Glasshouse

Declarations

Conflict of interest

The authors declare no competing interests.

Funding

This work was supported by the Guizhou Province High-level Innovative Talent Project (Grant No. Qiankehe Platform Talent-GCC [2022] 027 – 1), the Key Laboratory of Functional Agriculture of Guizhou Provincial Higher Education Institutions (Qianjiaoji [2023] 007), the Key Laboratory of Molecular Breeding for Grain and Oil Crops in Guizhou Province (Grant No. Qiankehe Zhongyindi [2023] 008), the Guizhou Provincial Science and Technology Plan Project (Grant No. Qiankehe Zhicheng [2025] Yiban 276), and the Guizhou Key Laboratory of High Quality, High Efficiency, and Yield Enhancement in Grain and Oil Crops (Grant No. Qian-Ke-He-Platform ZSYS[2025] 037).

Author Contribution

Conceptualization, BL, XLH and HBQ; methodology, XLH; software, HLW; validation, XMZ; investigation, BL and XLH; resources, HBQ and XMZ; data curation, BL; writing—original draft preparation, BL; writing—review and editing, HLW and XLH; project administration, HBQ; All authors have read and agreed to the published version of the manuscript.

Data Availability

The datasets generated and/or analyzed during the current study are available from the corresponding author on reasonable request.

References

1. Alameda, D., & Villar, R. (2009). Moderate soil compaction: Implications on growth and architecture in seedlings of 17 woody plant species. Soil and Tillage Research, 103(2), 325–331.

2. Allan, R. E., Vogel, O. A., & Peterson, C. J., Jr. (1962). Seedling emergence rate of fall-sown wheat and its association with plant height and coleoptile length. Agronomy Journal, 54(4), 347–350.
3. Bassett, I. E., Simcock, R. C., & Mitchell, N. D. (2005). Consequences of soil compaction for seedling establishment: Implications for natural regeneration and restoration. Austral Ecology, 30(8), 827–833.
4. Botta, G. F., Jorajuria, D., Balbuena, R., & Ressia, M. (2004). Tillage and traffic effects on soil compaction and sunflower (Helianthus annus L.) emergence. Soil & Tillage Research, 80(1-2), 79–86.
5. Brais, S. (2001). Persistence of soil compaction and effects on seedling growth in northwestern Quebec. Soil Science Society of America Journal, 65(4), 1263–1271.
6. Chou, H., Li, X., & Yu, J. (2021). China's corn industry: Development trends and policy recommendations. Issues in Agricultural Economy, (7), 4–16.
7. Colombi, T., Braun, S., Keller, T., & Walter, A. (2017). Artificial macropores attract crop roots and enhance plant productivity on compacted soils. Science of the Total Environment, 574, 1283–1293.
8. Dang, Z. P., Lei, L., & Liu, J. X. (2016). Application status and development path of corn mechanical direct harvesting technology. China Seed Industry, (4), 16–18.
9. Du, J. Y., Zhang, G. R., Cai, A. J., Liu, Y. F., Gao, G. H., & Jin, Z. Z. (2008). Study on the relationship between mesocotyl length and endogenous hormones in maize. Journal of Maize Sciences, 26(3), 70–73.
10. Dungan, G. H. (1950). Response of corn to extremely deep planting. Agronomy Journal, 42(5), 256–257.
11. Han, Q., Shen, Y., Lv, L., Lee, M., Lübberstedt, T., & Zhao, G. (2020). QTL analysis of deep-sowing tolerance during seed germination in the maize IBM Syn4 RIL population. Plant Breeding, 139(6), 1125–1134.
12. Han, Z. Y., Zhang, J. H., Bai, Y. G., Zheng, M., Liu, H. B., Xiao, J., ... & Zhao, J. H. (2022). Effects of soil amendments on soil properties and emergence rate under the 'dry sowing and wet emergence' mode in cotton fields of southern Xinjiang. Water Saving Irrigation, (8), 46–52+59.
13. Hoshikawa, K. (1969). Underground organs of the seedlings and the systematics of Gramineae. Botanical Gazette, 130(3), 192–203.
14. Li, H., Ribaut, J. M., Li, Z., & Wang, J. (2008). Inclusive composite interval mapping (ICIM) for digenic epistasis of quantitative traits in biparental populations. Theoretical and Applied Genetics, 116(2), 243–260.
15. Li, H., Ye, G., & Wang, J. (2007). A modified algorithm for the improvement of composite interval mapping. Genetics, 175(1), 361–374.
16. Li, X. Y., Tang, H. T., Liu, G., Zhang, B., Kang, J. W., & Mei, B. R. (2016). Discussion on maize production and breeding techniques in mountainous areas of southwest China. Agricultural Technology & Equipment, (5), 31–33+36.

17. Liu, H., Zhang, L., Wang, J., Li, C., Zeng, X., Xie, S., ... & Zhao, G. (2017). Quantitative trait locus analysis for deep-sowing germination ability in the maize IBM Syn10 DH population. Frontiers in Plant Science, 8, 813.
18. Luo, W. X., Tang, H. T., Xie, Y. C., Li, X. Y., Mei, B. R., Liu, G., & Kang, J. W. (2017). Analysis of maize growth adversity in southwest ecological region. Agricultural Science and Technology Communication, (8), 12–15.
19. Stuber, C. W., Edwards, M. D., & Wendel, J. F. (1987). Molecular marker-facilitated investigations of quantitative trait loci in maize. II. Factors influencing yield and its component traits. Crop Science, 27(4), 639–648.
20. Sun, Q., Li, T. Y., Li, D. D., Wang, Z. Y., Li, S., Li, D. P., ... & Wang, L. (2019). Overexpression of the maize ZmCOL9 gene improves seedling vigor and confers deep-seeding tolerance by regulating mesocotyl elongation in transgenic maize. Frontiers in Plant Science, 10, 1479.
21. Tuberosa, R., Sanguineti, M. C., Landi, P., Salvi, S., Casarini, E., & Conti, S. (1998). RFLP mapping of quantitative trait loci controlling abscisic acid concentration in leaves of drought-stressed maize (Zea mays L.). Theoretical and Applied Genetics, 97, 744–755.
22. Wang, J. (2009). Inclusive composite interval mapping of quantitative trait genes. Acta Agronomica Sinica, 35(2), 239–245.
23. Wang, X. Y. (2018). Harm of soil compaction and prevention measures. Agriculture in Henan, (5), 19+21.
24. Whalley, W. R., Finch-Savage, W. E., Cope, R. E., Rowse, H. R., & Bird, N. R. A. (1999). The response of carrot (Daucus carota L.) and onion (Allium cepa L.) seedlings to mechanical impedance and water stress at emergence. European Journal of Agronomy, 11(1), 1–12.
25. Wu, Z. W., & Lu, Y. C. (2020). Research progress on the application of SSR markers in maize research. Anhui Agricultural Bulletin, (Z1), 13–15.
26. Xu, J. Y., Wang, X. S., Yu, C. K., Wu, B., Ma, J., & Sun, J. C. (2015). Study on the survival and propagation habits of weedy rice in Ningxia II: Identification of seedling emergence ability and overwintering ability of weedy rice seeds. Seed, 34(11), 88–90.
27. Ye, H. (2019). Study on the effect of ZmMYB59 gene overexpression on the germination of maize seed top soil [Master's thesis, Zhejiang Agriculture and Forestry University].
28. Zhang, G. H., Lin, J. R., Wu, M. G., Cao, L. Y., & Cheng, S. H. (2005). Study on the power source of rice seedling top soil. Chinese Journal of Rice Science, (1), 61–64.
29. Zhang, H., Ma, P., Zhao, Z., Zhao, G., Tian, B., Wang, J., & Wang, G. (2012). Mapping QTL controlling maize deep-seeding tolerance-related traits and confirmation of a major QTL for mesocotyl length. Theoretical and Applied Genetics, 124(1), 223–232.
30. Zhang, L., Liu, Z. Z., Huang, Y. Q., Chen, J. T., & Zhu, L. Y. (2007). Analysis of deep sowing tolerance characteristics of 46 maize inbred lines. Journal of Hebei Agricultural University, 30(3), 18–21.

Tables

Tables 1 to 10 are available in the Supplementary Files section.

Figures

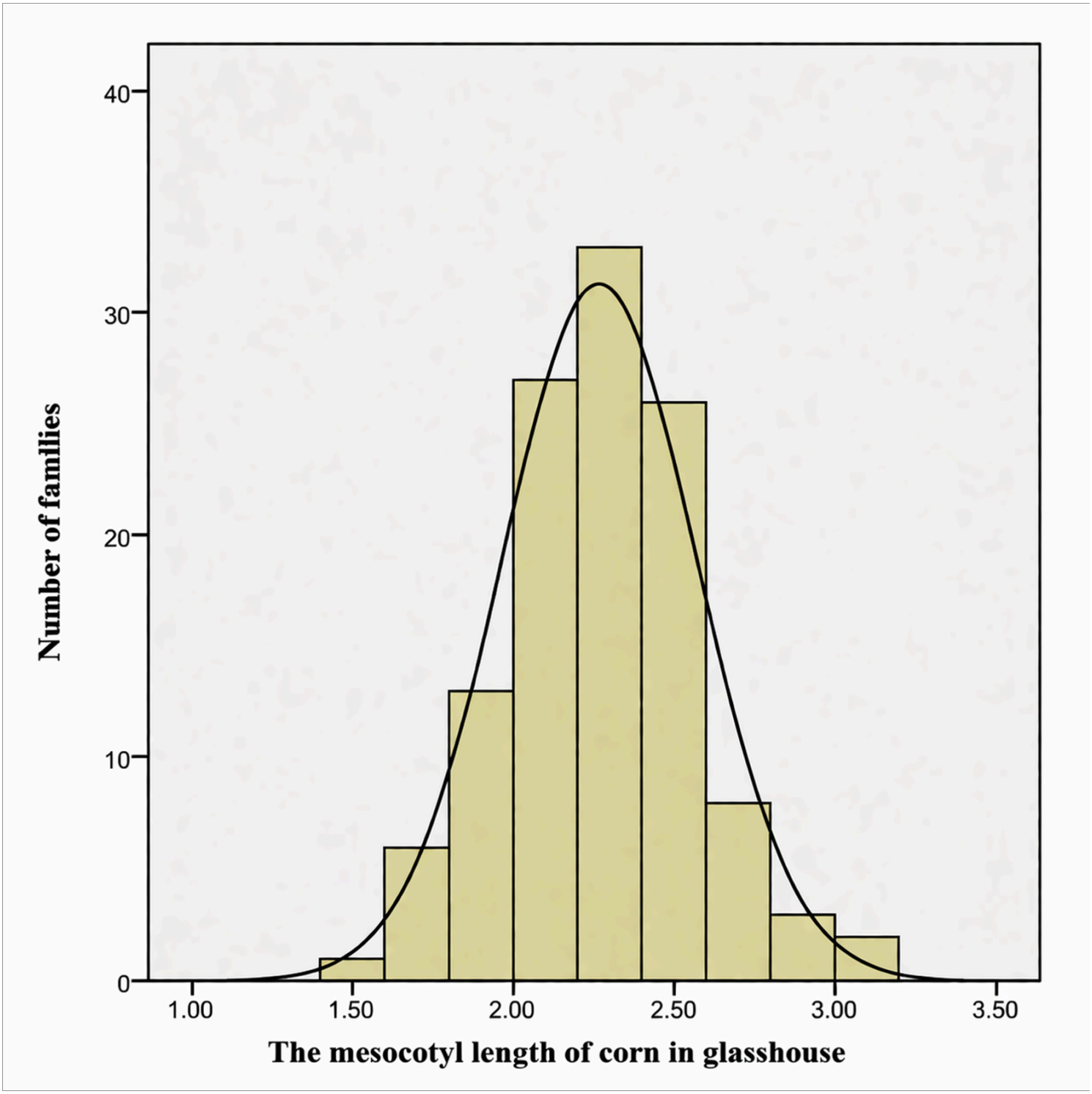


Figure 1

Legend not included with this version.

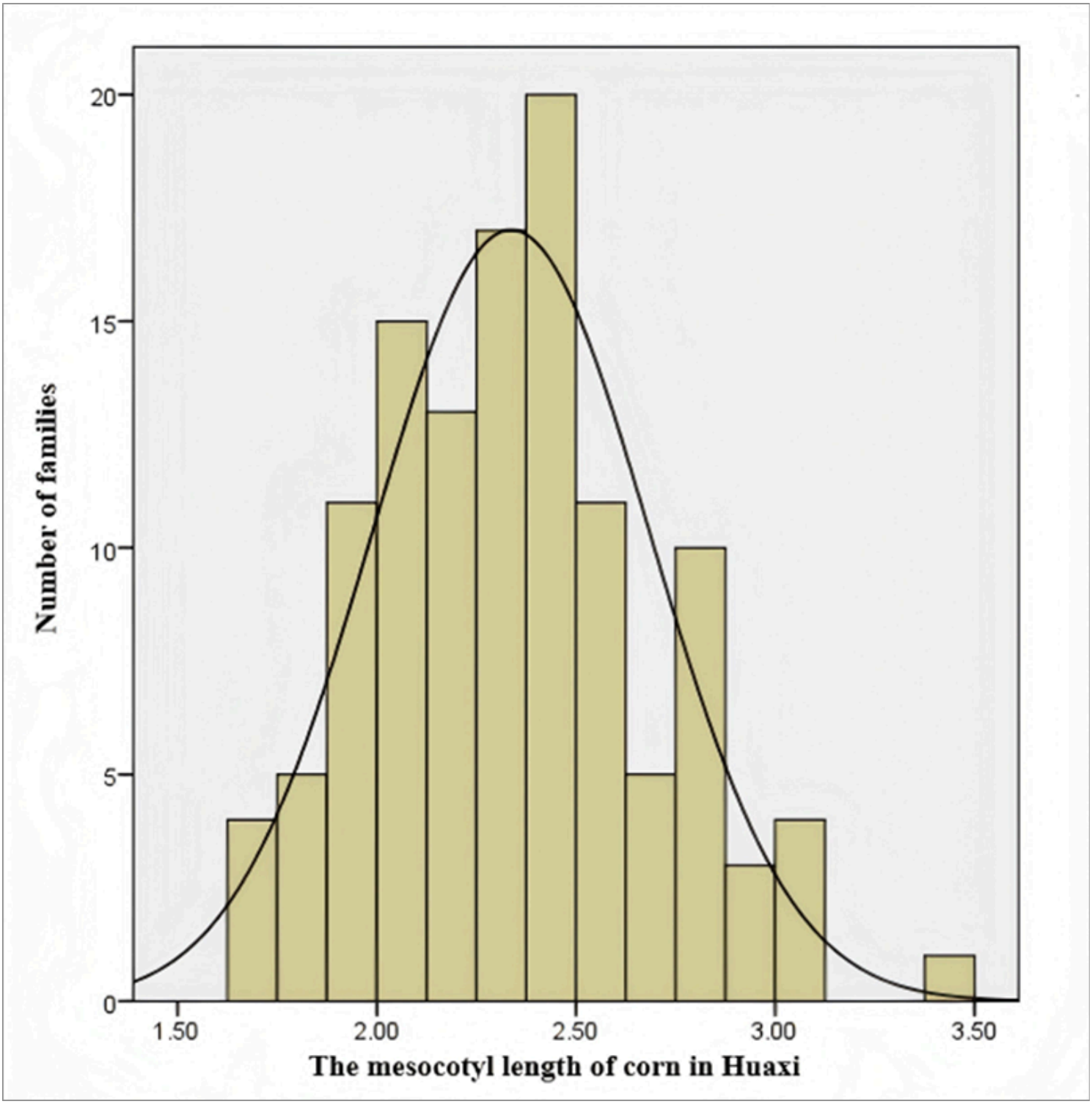


Figure 2

Legend not included with this version.

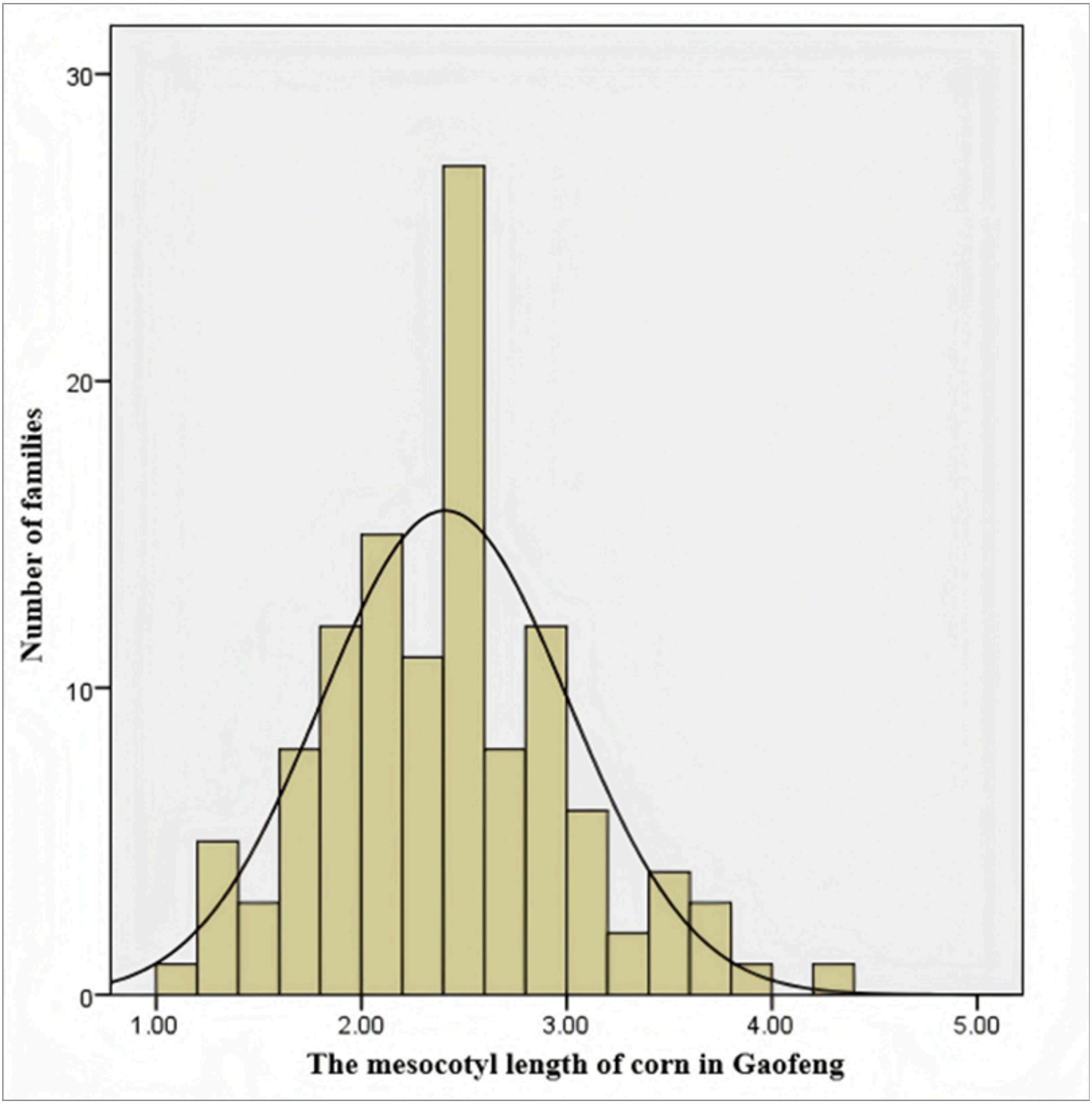


Figure 3

Legend not included with this version.

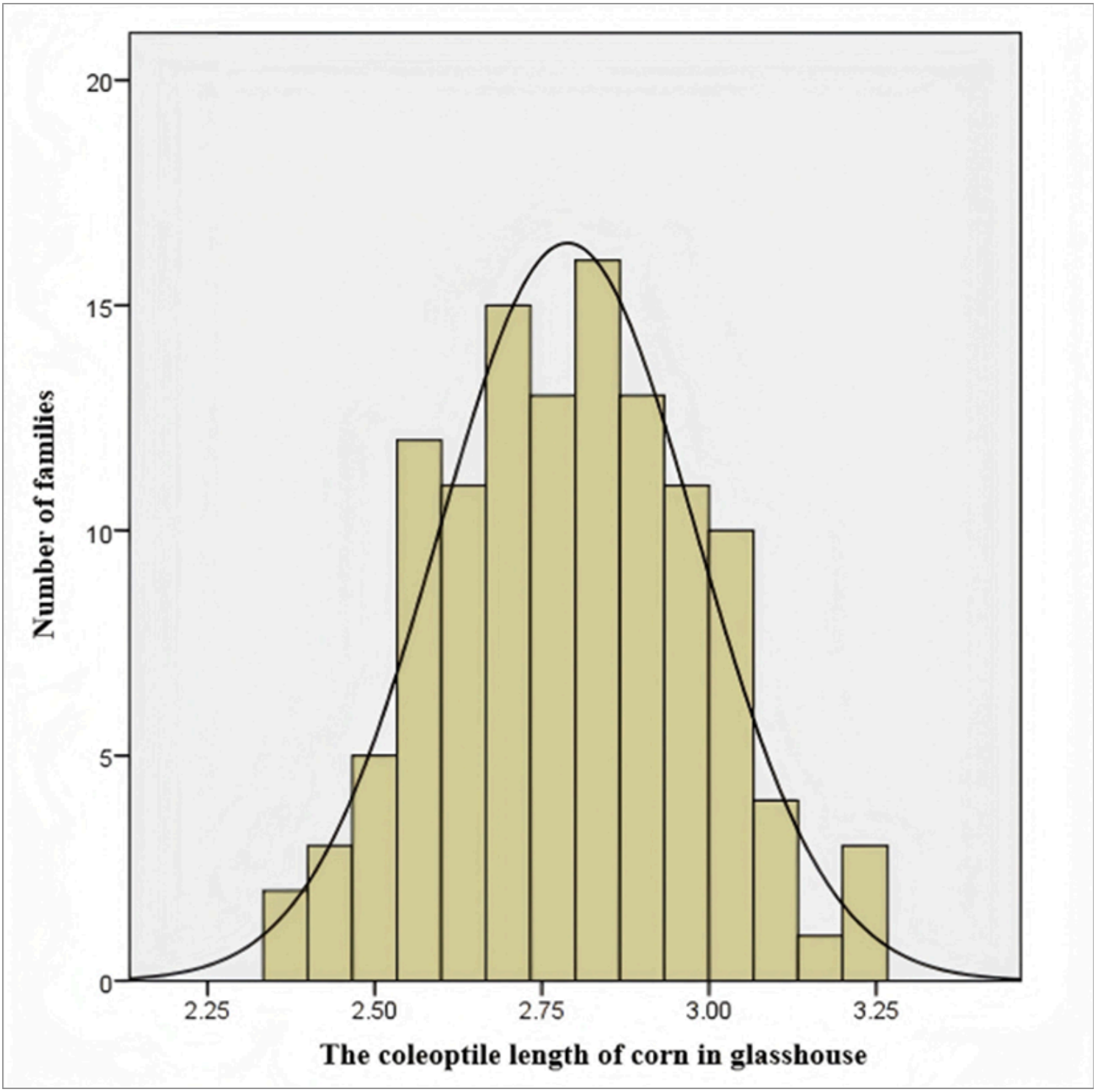


Figure 4

Legend not included with this version.

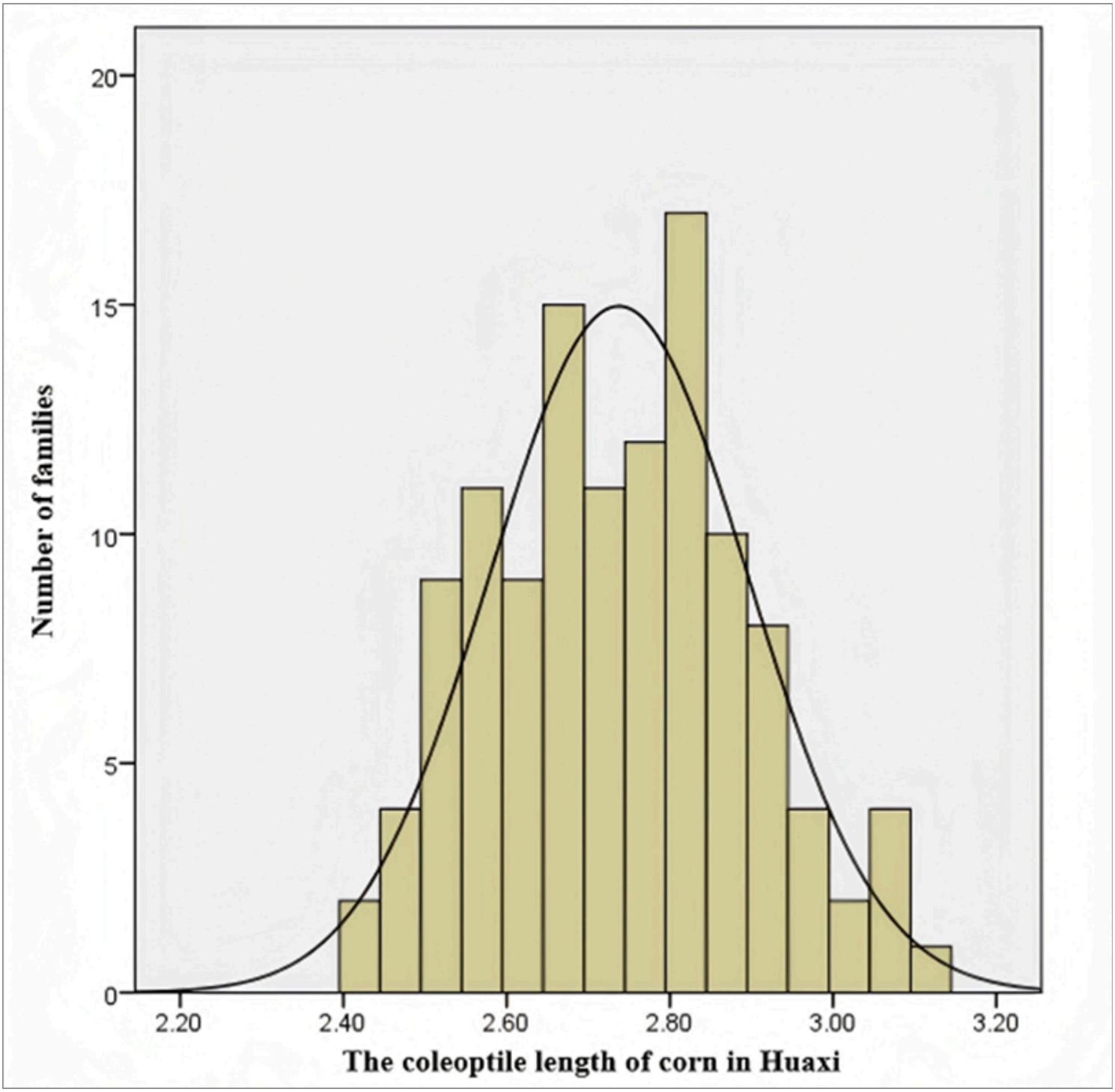


Figure 5

Legend not included with this version.

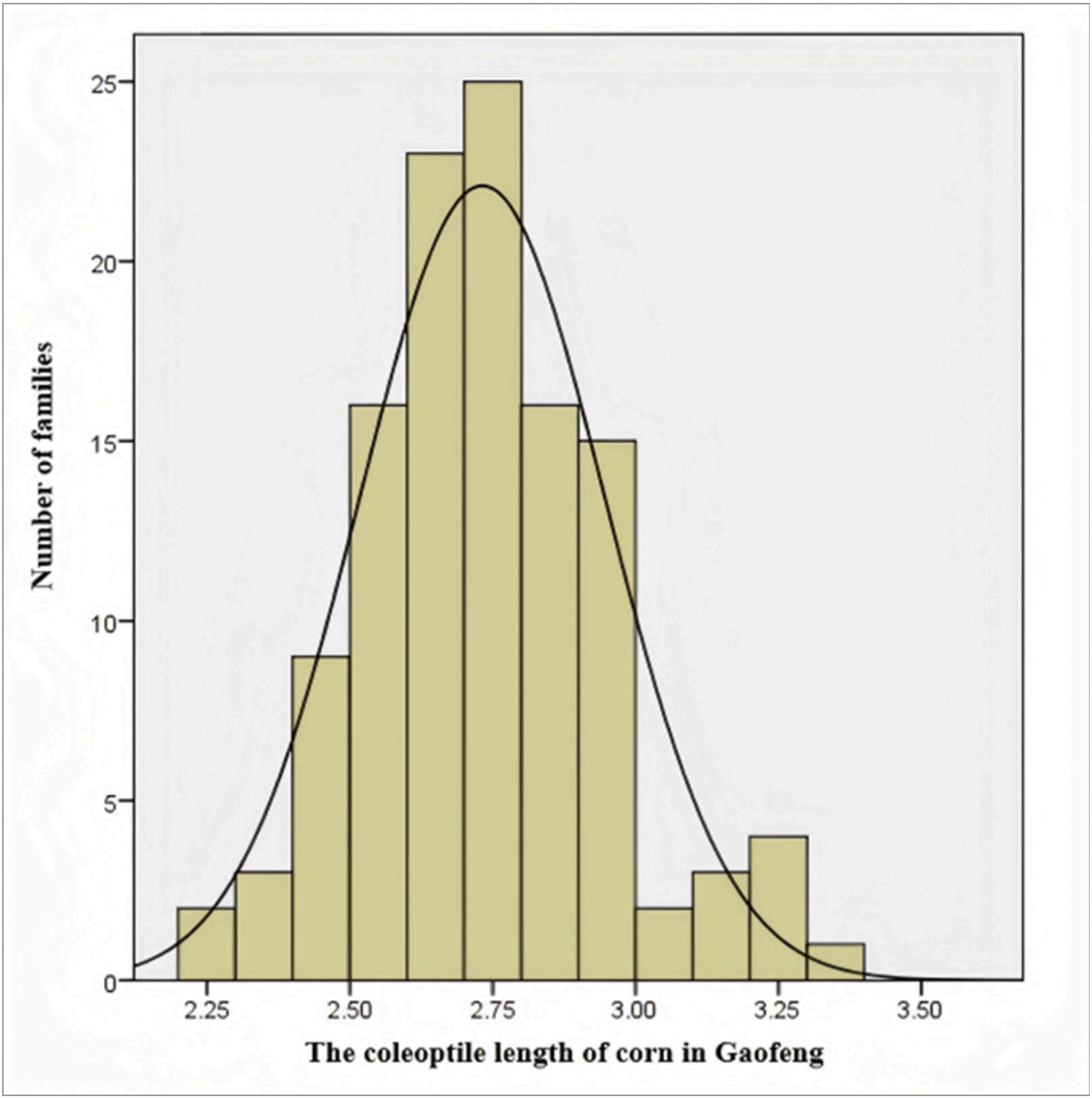


Figure 6

Legend not included with this version.

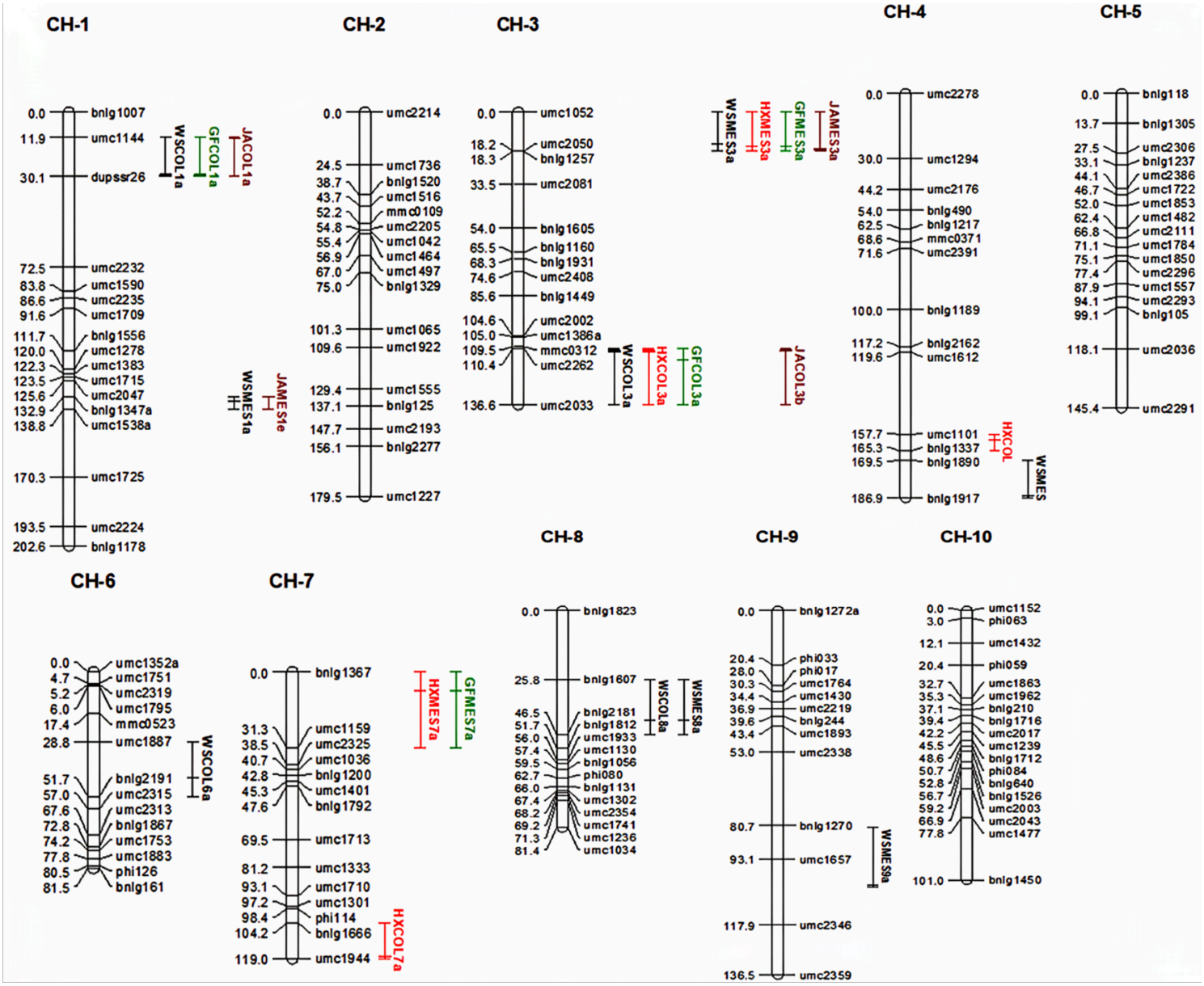


Figure 7

Legend not included with this version.

Supplementary Files

This is a list of supplementary files associated with this preprint. Click to download.

- Tables1and2.docx
- Table3.docx
- Tables4and5.docx
- Table6.docx
- Tables7and8.docx

- Tables9and10.docx